مؤتمر الأزهر الهندسي الدولي التاسع

AL-AZHAR ENGINEERING

NINTH INTERNATIONAL CONFERENCE

*April 12 - 14, 2007*

CODE:M44

# EXPERIMENTAL AND NUMERICAL STUDY OF FORCED CONVECTION HEAT TRANSFER FROM AN INCLINED HEATED PLATE PLACED BENEATH A POROUS MEDIUM

**A. R. EL-SHAMY[*], R. Y. SAKR[*], N. S. BERBISH[*], AND M. H. MESSRA[**]**

*Mech. Eng. Dept., Shoubra Faculty of Eng., Benha Univ., Egypt

**M.Sc. Student, Mech. Eng. Dept., Shoubra Faculty of Eng., Benha Univ., Egypt

## ABSTRACT

The aim of the present work is an experimental and numerical study of forced convection heat transfer from an inclined heated plate placed beneath a porous medium. The experiments were carried out on an aluminum flat plate of 320 mm length, 140 mm width, and 6 mm thickness and the plate was electrically heated with a uniform heat flux condition. The tested heated plate was inclined on the flow direction with different angles of attack ($\alpha$) varied from $0^o$ (horizontal position) to $30^o$, within a range of Reynolds number (based on the test plate length) from 52000 to 171000. The porous media used in the experiments were made of PVC, glass, and stainless steel materials, covering a wide range of solid thermal conductivities. The nominal sphere diameter of all used materials was nearly about 12 mm, and the porosity of the porous media was about 0.52. Also, the present problem was solved numerically using a commercial CFD code. Two cases have been investigated; flat plate without porous media and with porous media. Both cases were solved in two dimensions. The case of smooth plate without porous media utilized the standard k-$\varepsilon$ model to model the flow of air over the plate, but the laminar model was used to predict the case of plate with porous media. For plate with or without porous medium and the same inclination angle, the experimental results showed that the heat transfer coefficient was increased with increasing the Reynolds number. Also, it was found that the heat transfer coefficient was increased with increasing the inclination angle, and was reached the maximum enhancement ratio at inclination angle of $20^o$ and with further inclination of the heating plate ($20^o < \alpha \leq 30^o$), the heat transfer coefficient was slightly decreased. Moreover, it was observed that the existence of the packed bed increases the heat transfer coefficient. In addition, for a constant particle size, higher heat transfer coefficients were obtained with higher particle thermal conductivity (steel spheres). For smooth inclined plate without porous medium, the maximum average Nusselt number enhancement ratio (average Nusselt number of the inclined smooth plate/average Nusselt number of the horizontal smooth plate without porous media), $\overline{Nu}_{sm}/\overline{Nu}_o$, was about 1.239 and was obtained at $\alpha = 20^o$ and Re = 71927. Also, for the inclined plate with porous medium, the maximum enhancement ratio of the average Nusselt number ($\overline{Nu}_p/\overline{Nu}_o$) was about 3.10.

This value was obtained at $\alpha = 20^o$, Re=71927, and using stainless steel spheres porous medium. Good agreement was observed between the experimental data and the numerical results that obtained from the models in the range of ($0^o \leq \alpha \leq 20^o$) and for the all range of Reynolds number used in this study. Finally, empirical correlation for the average Nusselt number was obtained utilizing the present experimental data as a function of the Reynolds number, the inclination angle (angle of attack), and the thermal conductivity of the packing material.

**KEYWORDS: Forced Convection Heat Transfer, Inclined, Heated Flat Plate, Porous Medium.**

## 1. INTRODUCTION

Recently, flat plate solar collectors play an important role in utilizing solar energy for most of domestic and industrial applications. Therefore, progress toward improvement and modifications of this type of solar collectors is now urgent. One of the most parameters that affect the performance of a flat plate solar collector is the convective heat lost from the top glass cover to the wind. Also, precise determination of the convective heat transfer coefficient from the inclined top glass cover of a flat plate solar collector is more important. Sparrow and Tien [1] investigated experimentally the forced convection heat transfer at an inclined and yawed square plate. The results showed that, the measured heat transfer coefficients were found to be insensitive to the angle of attack. Imura et al. [2] carried out an experimental investigation to study heat transfer and buoyancy induced transition from laminar forced convection to turbulent free convection over a horizontal isothermally heated plate. The flow over a horizontal isothermally heated plate was characterized by a region of laminar forced convection near the leading edge, followed by the onset of longitudinal vortices and finally a transition to a turbulent flow regime. El-Sayed [3] studied experimentally the heat transfer from an inclined flat plate under uniform heat flux condition. The heated plate was made of brass material, and was situated at various orientations to the air flow direction within Reynolds number (based on test plate length) ranged from 78500 to 230000. Motwani et al. [4] carried out an experimental study to determine the average heat transfer coefficient during forced convection air flow over inclined and yawed rectangular plates. The experiments were performed under a constant surface temperature condition and covered two plates with two different aspect ratios of 2/3 and 1.5 respectively. The angle of attack was varied from 0 to 45 deg and the angle of yaw was varied from 0 to 30 deg. Also, the Reynolds number was varied from $0.2x10^5$ to $3.5x10^5$. Shalaby et al. [5] investigated experimentally forced convection heat transfer of air at an inclined and yawed rectangular plate. The experiments covered angles of attack from 0 to 45 deg, angles of yaw from 0 to 45 deg, and Reynolds number from 68000 to 220000 under constant surface temperature condition. The results show that the average Nusselt number decreases as the angle of attack increases from 0 to 15 deg and as increases from 15 to 45 deg; the decrease in Nusselt number values becomes insignificant. On the other hand Nusselt number values have a considerable change with the angle of yaw in each case. Shalaby and Araid [6] studied experimentally the average heat transfer coefficients during forced convection air flow over reversed rectangular flat plate. The experiments were carried out for constant surface temperature and covered reverse angles ($\gamma$) form 0 to 60 deg. El-Shamy [7] studied experimentally heat transfer to air flowing over an inclined flat plate within a range of Reynolds number from 30000 to 250000. Experiments were performed either at uniform heat flux or uniform surface temperature of the plate, as required. It was observed that the local heat transfer coefficient started with a relatively high value and it decreased gradually in the down-stream direction. However, before the end of the heating surface the local coefficient was increased again. El-Shamy [8] performed experimentally the effect of the presence of ribs on heat transfer in a turbulent flow of air over a horizontal flat plate. The

heating plate was made of brass material and was electrically heated under uniform heat flux condition within a range of Reynolds number from 50000 to 550000. The plate roughness was produced by using rectangular brass ribs. It was found that, the average Nusselt number enhancement ratio was increased with increasing the roughness and independent of the free stream pressure gradient. Abdel-Moneim [9] carried out an experimental investigation to study the heat transfer from an inclined smooth flat plate to a turbulent flow of air within a range of Reynolds number from $9.0x10^4$ to $9.0x10^5$. A brass plate was used as a heating surface and was electrically heated with a uniform heat flux. It was found that the heat transfer coefficient decreases with increasing the inclination angle and after a certain inclination angles, depends on the flow velocity, the heat transfer coefficient begins to increase with further inclination of the plate**.** Abdel-Moneim et al. [10] extended the work of El-Shamy [8]. Afify et al. [11] studied experimentally and theoretically the effect of free-stream turbulence on turbulent boundary layer drag reduction and heat transfer enhancement over plates with/without longitudinal V-micro-grooves. Three test plates, one smooth and two with triangular profile grooves having aspect ratios (groove height/pitch) of 0.7 and 1.3, were investigated within Reynolds number ranged from $1.2x10^5$ to $8.5x10^5$. The results indicate that V-micro grooves can enhance the convective heat transfer by as much as 25% compared with the smooth surface without a penalty of increasing the drag. Kamal et al. [12] carried out an experimental investigation to analyze the effect of an oblique multi circular air jets impingement on the flow fields and drying rates from a flat surface. It was found that the jets inclination angle of 60 deg is the optimum case which satisfies the largest drying rates beside the uniform pressure distributions along the drying plane.

The number of investigations on convective heat transfer through a fluid-saturated porous medium has been on the rise during the past decade. Many thermal engineering systems are in need of a better understanding of forced convection through porous materials. Such applications include: building thermal insulations, compact thermal collector-storage systems, drying processes, heat exchangers, grain storage, and catalytic reactors. The boundary and inertia effects in porous media forced convective heat transfer from a flat plate were first analyzed by Vafai and Tien [13] for a constant porosity medium. These effects were shown to play a significant role in highly permeable medium, high Prandtl number fluids, and fast flows. A similar study was reported recently by Beckermann and Viskanta [14] and Vafai and Thiyagaraja [15]. For the case of a fully developed momentum boundary layer, a closed form analytical solution for the velocity profile and an approximate solution for the thermal boundary-layer thickness and the local Nusselt number were obtained by the former. The investigations note that porosity variations near the wall, for example, in packed beds of spheres, will alter the results considerably due to the channeling of the flow near the wall. The works of Vafai [16] and Vafai et al. [17] document theoretically the effect of flow channeling on flat plate forced convection, while Poulikakos and Renken [18] and Renken and Poulikakos [19] thoroughly investigate this phenomenon for forced convection at the thermal entry and fully developed regions in a channel filled with a porous medium. Kaviany [20] studied theoretically the effect of the presence of an isotropic solid matrix on the forced convection heat transfer rate from a flat plate using the integral method. Renken and Poulikakos [21] studied experimentally the forced convection from a horizontal heated plate (Aluminum alloy) which constructs the upper surface of a channel filled with glass spheres with a measured pore porosity of 0.39. It was observed that the temperature in the porous bed decreases monotonically as we move away from the heated plate. Nakayama et al. [22] studied theoretically non-Darcian flow and heat transfer through a boundary layer developed over a horizontal flat plate embedded in a fluid-saturated porous-medium using the local similarity solution procedure. The convective inertia effect appears on the velocity and

temperature profiles in the boundary layer developing region. In the downstream region, the porous inertia becomes appreciable on the velocity profile, but its effect on the temperature profile seems insignificant. Afify and Berbish [23] studied experimentally the forced convection heat transfer over a horizontal heated Aluminium flat plate placed beneath a porous medium of spherical particles. The porous media used in the experiments were made of glass, rock, and steel materials. With air as the working fluid, the experiments have been made under the condition of constant heat flux for Reynolds number ranging from $10^5$ to $10^6$. It was found that the local and average heat transfer coefficients were increased with increasing the Reynolds number, particle diameter, and particle thermal conductivity. Luna and Mendez [24] conducted a theoretical investigation to study the heat transfer process for the hydro-dynamically developed forced convection flow on a heated flat plate embedded in a porous medium. The predictions for the temperature profile of the plate and the local and average Nusselt numbers were obtained.

The main purpose of the present work is to investigate numerically and experimentally forced convection heat transfer from a flat plate at various orientations placed beneath a porous medium of spherical particles. Several packing materials, encompassing a wide range of thermal conductivities, have been employed with air as the working fluid at different Reynolds numbers, in order to generate a large data base. Empirical correlation for the average Nusselt number was obtained as a function of Reynolds number, angle of attack, and solid-to-fluid thermal conductivity ratio.

## 2. EXPERIMENTAL SET-UP AND MEASURING INSTRUMENTS

The measurements were carried out in an open-loop air flow circuit in suction mode of a relatively low turbulence level wind tunnel. The experimental set up is shown schematically in Fig.(1). It comprises the following major components: air passage, test section, measuring instruments, and power supply with associated controls. The purpose of the air passage is to supply the air to the test section, and it consists of the following: bell-mouth intake, honey comb section, main duct, transformation duct, and air blower. The main duct, which supplies air to the test section, is a horizontal square duct having dimensions of 300 mm x 300 mm, and its length is 1300 mm. The air flow discharge is controlled at the air blower outlet by means of a variable outlet area using adjustable gate, where the air is exhausted into the atmosphere. The porous medium has approximate dimensions of 340 mm length, 145 mm width, and 60 mm height. The packed beds are poured randomly inside the test section cage until it is filled. The porous media used in the experiments are packed beds of solid spheres made of PVC, glass, and stainless steel materials, covering a wide range of solid thermal conductivities. The spheres diameter of the porous media is 12 mm. The bulk porosity of the whole porous media is nearly about 0.52. The construction of the heating unit is shown in Fig.(2), and it consists of the heating plate, the main and guard heaters, asbestos between the two heaters, heater insulation and wooden frame. The heating surface was made of a highly polished aluminum plate having dimensions of 320 mm length, 140 mm width, and 6 mm thickness. The heated test plate was placed at a distance of 1500 mm from the beginning of the working section. The particles of the porous medium were placed over the heated flat plate. The air stream over the tested flat plate was heated, under uniform heat flux conditions, by means of an electrical heater. The total heat liberated from the main heater was given to the air stream by eliminating the different losses. The main heater was made of nickel-chromium heating tape of 5 mm width, 0.2 mm thickness, and 3.8 Ω/m electric resistance. The heating tape was wound around a mica sheet of 320 mm x 140 mm x 0.5 mm with a uniform pitch of 10 mm and placed between two mica sheets of the same size. The total resistance of the main heater is 39 Ω. Also, a guard heater, similar to the main heater, was used to establish thermal equilibrium in the asbestos layer placed between the main and guard

heaters. Asbestos sheets were used to thermally insulate the heating unit and a wooden frame was also used to hold all the heating elements with its asbestos insulation section, as shown in Fig.(2). The heating surface was placed in the same plane of the horizontal lower wall of the working section in order to avoid any eddies over the test plate. The heating unit was fixed at the front edge with two copper hinges. The rear edge of the heating unit is attached to a mechanism designed to permit the plate to be set at any desired angle. There was a scale used for measuring the plate inclination angle ($\alpha$). The free-stream temperature, $T_\infty$, of the air was taken as the average of the readings of two thermocouples located at the center-line of the wind tunnel upstream of the test plate. Digital turbine air flow meter with a minimum reading of 0.01 m/s was used to measure the air velocity inside the duct at the inlet to the test section. The surface temperatures of the heated plate were measured using seventeen calibrated chromel-alumel (0.2 mm wire diameter) thermocouples. The thermocouples were welded to the back surface of the test plate and distributed along the length and across the span of the test plate (thirteen along the length and four across the span). In addition, three pairs of similar thermocouples were oppositely fixed at equal distance on the two sides of the asbestos sheet which was inserted between the main and the guard heaters. The temperatures were indicated by using a digital thermometer connected to the thermocouples leads via selector switches with a minimum reading of 0.1 $^oC$. The electric power inputs to the main and guard heaters were determined separately by measuring both the voltage drop and the electric resistance for each heater. Two variac transformers were used to adjust the heating power for the main and the guard heaters by varying the input voltages to the heaters. The voltage drop and the electric resistance for each of the main and guard heaters were measured by a digital multimeter, with minimum readings of 0.1 Volt and 1Ohm.

## 3. EXPERIMENTAL PROCEDURE AND METHOD OF CALCULATIONS

The bulk porosity ($\pi$) of the porous medium was computed from the following equation:

$$\pi = (V_t - V_p)/V_t \qquad (1)$$

where; $V_p$ is the volume of the particles and $V_t$ is the total volume of the porous media test section.

The main heater variac transformer was fixed at a particular voltage and the guard heater input was regulated to insure thermal equilibrium in the asbestos layer placed between the main and the guard heaters. This was established when the temperature difference between the asbestos-layer surfaces becomes less than 0.5 $^oC$. After steady state conditions were achieved, the thermocouples readings were recorded and the local heat transfer coefficient was calculated by,

$$h_x = \frac{q_t - q_{Loss}}{A(T_w(x) - T_\infty)} \qquad (2)$$

The electrical power generated from the main heater, $q_t$, was determined from the measured voltage and the measured main heater resistance as;

$$q_t = \frac{V_m^2 \cos\phi}{R_m} \qquad (3)$$

The power factor, Cos $\phi$, was 0.98 for the present resistive load (heaters). Also, the total heat lost by radiation to the surroundings and by conduction through the insulation layers was calculated within the tested range of parameters. The local Nusselt number based on the plate length and the fluid thermal conductivity was calculated as:

$$Nu_x = \frac{h_x L}{k_f} \qquad (4)$$

Also, the average heat transfer coefficient and the corresponding average Nusselt number were calculated at different flow velocities and at different angles of attack as:

$$\bar{h} = \frac{1}{L}\int_0^L h_x dx \quad \text{and} \qquad \overline{Nu} = \frac{\bar{h}L}{k_f} \tag{5}$$

## 4. UNCERTAINTY ANALYSIS

Generally, the accuracy of the experimental results was governed by the accuracy of the individual measuring instruments. Also, the accuracy of an instrument was limited by its minimum division (its sensitivity). In the present work, the uncertainties in both the heat transfer coefficient (Nusselt number) and in the flow velocity (Reynolds number) were estimated by following the differential approximation method. The total uncertainty in measuring the main heater input voltage, the main heater electric resistance, the air temperature ($T_\infty$), the heating surface temperature ($T_w$), and the plate surface area (A) were 1.923%, 0.256%, 0.333%, 0.333%, and 1.027% respectively. These were combined to give a maximum overall error of 3.872% in the reported heat transfer coefficient or Nusselt number. Also, uncertainty of 1.0% was found in measuring the flow velocity or reported Reynolds number.

## 5. CFD MODELLING

### 5.1. Basic equations for flat plate without porous media

The flow field to be analyzed is governed by the Navier-Stockes, continuity, and energy equations. These equations are closed using two-equation k-ε turbulence model. These equations are expressed in terms of partial differential equations (PDE's). These PDE's are discretized using the finite volume technique. The general form of momentum, energy, species, and turbulent model equations are all similar and can be expressed into a common scalar transport form:

$$\frac{\partial(\rho\phi)}{\partial t} + \frac{\partial(\rho u\phi)}{\partial x} + \frac{\partial(\rho v\phi)}{\partial y} + \frac{\partial(\rho w\phi)}{\partial z} = \frac{\partial}{\partial x}\left(\Gamma_\phi \frac{\partial \phi}{\partial x} - \overline{\rho u'\phi'}\right) + \frac{\partial}{\partial y}\left(\Gamma_\phi \frac{\partial \phi}{\partial y} - \overline{\rho v'\phi'}\right) + \frac{\partial}{\partial z}\left(\Gamma_\phi \frac{\partial \phi}{\partial z} - \overline{\rho w'\phi'}\right) + S_\phi \tag{6}$$

where; $\phi$: dependent variable (u, v, w, T, k, ε); $\phi$=1 (continuity)

$S_\phi$: source/sink term

$\Gamma_\phi$: diffusion coefficient.

$\overline{\rho u'\phi'}$, $\overline{\rho v'\phi'}$ and $\overline{\rho w'\phi'}$ **:** Reynolds stresses

The Reynolds stresses are related to the mean flow quantities via k-ε turbulence model**.** The transport equations of this model have been discussed numerous times in the literature, so the reader is referred to details in [25]. The CFD code used in the present paper solves the transport equations of 2-D, thermal incompressible turbulent flow in the Cartesian coordinates. Discretization is the process by which the PDE's are transformed into algebraic equations with the aid of the assumption on the spatial distribution of flow and fluid properties. The finite-volume method incorporated with quadratic upwind interpolation technique is employed to integrate and interpolate the PDE's represented by Eq.(6). It should be noted that this technique leads to a solving scheme which retains the conservative properties of the governing PDE's.

Using the segregated solver in the solution algorithm, the governing equations are solved sequentially. To obtain a converged solution, several iterations of the solution loop must be performed. In the segregated solution method, each discrete governing equation is linearized

implicitly with the equation's dependent variable. This will result in a system of linear equations for each cell in the domain. The standard k-ε model was used in the present work because its results corresponds better with the experimental data from the present work and the previous published correlations for the case of clear air.

## 5.2. Basic equations for flat plate with porous media

In this work, for the case of flat plate with porous media, steady 2-D laminar, non-Darcian, flow is analyzed. The flow and heat transfer are governed by the conservation of mass, momentum and energy equations as follows

a) Mass Conservation:

$$\frac{\partial(\rho u)}{\partial x}+\frac{\partial(\rho v)}{\partial y}=0 \qquad (7)$$

b) Momentum, flow in non-Darcian porous medium

$$\frac{\partial}{\partial x}\left(\rho u\frac{u}{\pi}\right)+\frac{\partial}{\partial y}\left(\rho v\frac{u}{\pi}\right)=-\frac{\partial p}{\partial x}+\frac{\partial}{\partial x}\left(\frac{\mu_B}{\pi}\frac{\partial u}{\partial x}\right)+\frac{\partial}{\partial y}\left(\frac{\mu_B}{\pi}\frac{\partial u}{\partial y}\right)-\left(\frac{1.75}{\sqrt{150}}\frac{\rho}{\sqrt{\pi^3 K}}|\vec{v}|+\frac{\mu}{K}\right)u \qquad (8a)$$

$$\frac{\partial}{\partial x}\left(\rho u\frac{v}{\pi}\right)+\frac{\partial}{\partial y}\left(\rho v\frac{v}{\pi}\right)=-\frac{\partial p}{\partial x}+\frac{\partial}{\partial x}\left(\frac{\mu_B}{\pi}\frac{\partial v}{\partial x}\right)+\frac{\partial}{\partial y}\left(\frac{\mu_B}{\pi}\frac{\partial v}{\partial y}\right)-\left(\frac{1.75}{\sqrt{150}}\frac{\rho}{\sqrt{\pi^3 K}}|\vec{v}|+\frac{\mu}{K}\right)v \qquad (8b)$$

c) Energy , assuming local thermal equillibrium between the solid and fluid phases

$$\rho_f cp_f\left(u\frac{\partial T}{\partial x}+v\frac{\partial T}{\partial y}\right)=k_{eff}\left(\frac{\partial^2 T}{\partial x^2}+\frac{\partial^2 T}{\partial y^2}\right) \qquad (9)$$

In the present CFD code, porous media is treated as a special type of fluid , and it requires to input the coefficients of the following Forchheimer equation [26,27]:

$$\frac{\Delta p}{L}=A\,\mu\,u+B\,\rho\,u^2 \qquad (10)$$

where A and B are termed as viscous and inertia coefficient and are given by:

$$A=1/K,\quad B=F/\sqrt{K}$$

The first coefficient A, has the dimension of $m^{-2}$ and the second coefficient B, has the dimension of $m^{-1}$ and K is the permeability of the porous media and is given by:

$$K=\frac{d_p^2\pi^3}{150(1-\pi)^2}$$

where F: is the Forchheimer coefficent.

Also, the laminer flow model was used because its results corresponds better with the experimental data obtained here.

## 5.3. Simulation geometry

The physical problem associated with the boundary conditions and grid are shown in Fig. (3a,b). The computational domain starts 300 mm before the test plate (320 mm) and extend 400 mm after it. Also, it is discretized with approximatly 6359 nodes, 2-D unstructured triangular mesh elements. More dense elements are made inside the porous layer zone. The convergence criterion adopted in the calculations was set so the normalized residual was less than $10^{-5}$ at any grid point for any $\phi$ equation.

## 6. RESULTS AND DISCUSSION

In the present work, the effects of Reynolds numbers, and particle thermal conductivity on heat transfer were investigated for different inclination angles. The porous media used in the present study were packed beds of solid spheres made of PVC, glass, and steel materials.

## 6.1. Test set-up evaluation

A preliminary series of experiments was carried out for the smooth flat plate in the horizontal position (at zero angle of attack) at different Reynolds numbers, to check the validity of the present experimental set-up, the measuring instruments and the computational model. The Reynolds number based on the plate length was varied from 52000 to 171000. The variations of the local Nusselt number ($Nu_x$) of the horizontal smooth plate versus the dimensionless axial distance X/L at different Reynolds numbers are shown in Fig.(4). It was observed that, the local Nusselt number takes a relatively high value near the leading edge of the plate and a steady decrease was obtained in the stream-wise direction consistent with a thermally developing flow until it reaches a constant value. Then, it remains constant or decreases slightly towards the trailing edge of the plate. Also, the average Nusselt number was calculated by integrating the local Nusselt number values along the plate length, and plotted versus the Reynolds number for $\alpha = 0^o$, as shown in Fig. (5). The average Nusselt number, which obtained from experiments, for the smooth horizontal plate ($\overline{Nu}_o$) was correlated as a function of Reynolds number by using the least square method and the following correlation was obtained:

$$\overline{Nu}_o = 0.13\,Re^{0.703} \qquad (11)$$

This correlation was valid within the present range of Reynolds number from 52000 to 171000 with a maximum deviation of ± 4.8%. Also, the numerical results were utilized to obtain the following correlation for the same case:

$$\overline{Nu}_o = 0.325\,Re^{0.6255} \qquad (12)$$

The present correlations, Eqs.(11-12) were compared with the available previous correlations [4, 7, 9 &10] and good agreement was found as shown in Fig.(5) and presented in Table (1). The good agreement between the present experimental and numerical results with the previous correlations ensures the reliability and the validity of the experimental set up, the method of calculations and the present computational code.

**Table (1): Comparison of the present and pervious correlations for smooth horizontal plate**

| Worker | Correlation | Range of Re | %Deviation* |
|---|---|---|---|
| Present – Experimental | $\overline{Nu}_o = 0.13\,Re^{0.703}$ | $0.52x10^5$- $1.71x10^5$ | ----- |
| Present– Numerical | $\overline{Nu}_o = 0.325Re^{0.6255}$ | $0.52x10^5$- $1.71x10^5$ | ----- |
| Motwani et al. [4] | $\overline{Nu}_o = 0.056\,Re^{0.77}$ | $0.2x10^5 – 3.5x10^5$ | 10% |
| El-Shamy [7] | $\overline{Nu}_o = 0.210\,Re^{0.66}$ | $0.5x10^5 – 5.5x10^5$ | 3.0% |
| Abdel-Moneim [9] | $\overline{Nu}_o = 0.657\,Re^{0.563}$ | $0.9x10^5 – 9.0x10^5$ | 9.0% |
| Abdel-Moneim et al. [10] | $\overline{Nu}_o = 0.437\,Re^{0.598}$ | $0.5x10^5$ - $10^6$ | 6.0% |

* $\%\,\text{Deviation} = (\overline{Nu}_{o,\,\text{previous}} - \overline{Nu}_{o,\,\text{present}}) / \overline{Nu}_{o,\,\text{previous}}\ x\,100$

## 6.2. Results of inclined smooth flat plate

Experiments were performed for different inclination angles of 5, 10, 15, 20, 25 and 30 deg., with air as the working fluid within a range of Reynolds number from 52000 to 171000. The local Nusselt number values were plotted versus the dimensionless axial location X/L for

different Reynolds numbers and at $\alpha = 20^o$, as shown in Fig.(6). The results showed that the local Nusselt number were increased near the plate trailing edge. This increase in the local values beyond to the thermal entrance length may be attributed to the increase in the flow velocity near the plate trailing edge due to the wind tunnel blockage especially at the higher angles of attack [7 & 9]. Figure (7) shows the variation of the average Nusselt number of smooth inclined plate ($\overline{Nu}_{sm}$) with the inclination angle ($\alpha$) at different Reynolds numbers. It was observed that, for experimental data, at the lower range of the angle of attack ($\alpha \leq 20^o$), the average Nusselt number increases with increasing the angle of attack. Also, at the higher values of the angle of attack ($20^o < \alpha \leq 30^o$) the average Nusselt number enhancement begins to decrease with further increase in the angle of attack. This decrease in the enhancement of the average Nusselt number with the angle of attack may be attributed to the generation of the turbulence decay zones over the inclined plate surface due to the main flow impact with the plate. But the numerical results show continuous increase of the average Nusselt number with the increase of the angle of inclination. Fig.(8) shows the variation of the average Nusselt number enhancement ratio (average Nusselt number for smooth inclined plate / average Nusselt number for smooth horizontal flat plate), $\overline{Nu}_{sm}/\overline{Nu}_o$, versus the angle of attack at different Reynolds numbers. The experimental results showed that the maximum average Nusselt number enhancement ratio was about 1.239, and was obtained at $\alpha = 20^o$ and Re = 71927.

Moreover, the average Nusselt number of the smooth inclined plate without porous medium ($\overline{Nu}_{sm}$) was correlated utilizing the present experimental data and numerical results respectively as a function of Reynolds number ( Re ) and the angle of attack ( $\alpha$ ) as follows:

$$\overline{Nu}_{sm} = 0.13\,Re^{0.703}\,(1+\sin\alpha)^{0.38} \qquad (13)$$

with a maximum deviation of about $\pm$ 8 %

$$\overline{Nu}_{sm} = 0.325\,Re^{0.6255}\,(1+\sin\alpha)^{0.5} \qquad (14)$$

with a maximum deviation of about $\pm$ 5 %

Both correlations were valid within the range of Reynolds number ($52000 \leq Re \leq 171000$), and the angle of attack ($0^o \leq \alpha \leq 20^o$). The present correlated experimental data, given by Eq.(13), is shown in Fig.(9). Also, the present correlations that given by Eqs.(13, 14) were compared with the available previous correlations at $\alpha = 20^o$ within the present experimental range of Re and the comparison is shown in Fig.(10). The good agreement between the present experimental results and the previous correlations provides considerable confidence in the accuracy of the data subsequently obtained with the porous media over the heated plate.

## 6.3. Results of inclined plate placed beneath a porous medium

The main objective of the present work is to study the effects of the Reynolds number, the plate inclination angle, and the particle thermal conductivity of the porous medium on forced convection heat transfer from an inclined heated plate placed beneath a packed layer of solid spheres. The porous media used in the experiments were packed beds of solid spheres of 12 mm diameter, and having materials of PVC, glass and stainless steel. The present results of the local Nusselt number for steel spheres porous medium at $\alpha = 0^o$ are shown in Fig.(11). The results show that the local Nusselt number decreases gradually from the leading edge of the tested plate, then it remains constant all over the downstream length of the plate in the flow direction. The previously published data of Afify and Berbish [23] of the local Nusselt number for steel spheres porous medium at $\alpha = 0^o$ are displayed for comparison and fair agreement was found as shown in Fig.(11). Also, the variations of the average Nusselt

number ($\overline{Nu}_p$) with Reynolds number at different inclination angles for PVC, glass, and stainless steel spheres, are shown in Figs.(12), (13), and (14) respectively. It was observed that the average Nusselt number increases with the increase of the angle of attack (α).

## 6.4. Effect of particle conductivity on heat transfer

To show the effect of particle thermal conductivity of the porous medium, three different materials namely PVC, glass, and stainless steel of constant spheres diameter, d =12 mm were studied. The variations of the local Nusselt number with dimensionless axial distance for the different materials of the porous media for $\alpha = 20^o$ and Re = 150745 are indicated in Fig.(15). Also, the average Nusselt number was plotted versus the angle of attack for the different materials of the porous media and for Re = 110690 as shown in Fig.(16). It was observed that the packed bed increases the Nusselt number greatly, indicating that the particles serve as effective enhancers for forced convection heat transfer. In addition, the packing material with a high thermal conductivity (stainless steel) has a higher heat transfer than material of approximately the same size but of low conductivity (PVC). This is due to the high thermal conductivity of steel, which results in high contact condition. Thus, it was concluded that for a constant particle size, an increase in particle conductivity yields an increase in the heat transfer. Moreover, the maximum enhancement ratio of the average Nusselt number (average Nusselt number of the inclined plate with porous media/average Nusselt number of the horizontal smooth plate without porous media), $\overline{Nu}_p / \overline{Nu}_o$, is about 3.10. This maximum enhancement ratio was obtained at $\alpha = 20^o$, Re = 71927 and using packed bed of steel spheres as indicated in Fig.(17).

## 6.5. Average Nusselt number correlation

The average Nusselt number for the inclined flat plate with porous media ($\overline{Nu}_p$) is correlated utilizing the present experimental data as a function of the Reynolds number (Re), the angle of attack (α), and the particle to fluid thermal conductivity ratio $(k_s / k_f)$ as follows :

$$\overline{Nu}_p = 0.13\,Re^{0.703}\,(1+\sin\alpha)^{0.38}\,(k_s/k_f)^n \qquad (15)$$

Where the constants were obtained by curve fitting based on a least-squares method through the present data. The exponent n = 0.1 for each of PVC and glass spheres, and n = 0.13 for stainless steel spheres porous medium were obtained. This correlation was valid within the present ranges of Reynolds number ($5.2x10^4 \le Re \le 1.71x\,10^5$), angle of attack ($0^o \le \alpha \le 20^o$), and the particle to fluid thermal conductivity ratio ($5.93 \le (k_s/k_f) \le 556$). The maximum deviation of the measured data from the above correlation, Eq.(15), is about ±9.5% as shown in Fig. (18).

Also, the obtained numerical results from the model were utilized to get the following correlation:

$$\overline{Nu}_p = 0.108\,Re^{0.707}\,(1+\sin\alpha)^{0.678}\,(k_s/k_f)^{0.143} \qquad (16)$$

for the same ranges used in the experiments for Reynolds number, inclination angle, and thermal conductivity ratio.

## 6.6. Fluid flow and heat transfer characteristics

The effect of Reynolds number on the fluid flow and heat transfer characteristics, represented by stream function and temperature contours, for the case of PVC porous spheres and α=0, is depicted in Fig.(19). It is noticed that as Re increases the stream function (left) increases, but the flow characteristics is unchanged. Also, it is observed on the right side that as Re

increases the thermal boundary layer thickness decreases indicating for more increase in the heat transfer as reported before for the average Nusselt number results.

The effect of the inclination angle on fluid flow and heat transfer characteristics, represented by stream function and temperature contours, for the case of glass porous spheres and Re=110690, is illustrated in Fig. (20). It is noticed that at this value of Re number, a single cell behind the heated inclined plate is formed at $\alpha \geq 20^o$ (left side). On the right side, the temperature contours show that the increase in the inclination angle results in slight decrease of the thermal boundary layer over the plate, thus increase the rate of heat transfer. Also, it is observed that behind the heated inclined plate, a zone of higher temperature (single cell zone) than the free stream is created. Figure (21) shows the effect of porous media's particles material on fluid flow and heat transfer characteristics, represented by stream function and temperature contours, for the case of $\alpha$=0 and Re=110690. It is noticed that for case of steel particles porous medium, the flow and heat transfer characteristics are different from those for PVC and glass and this may be due to the higher difference between the density and the thermal conductivity of steel compared with PVC and glass.

## 7. CONCLUSIONS

In the present work, forced convection heat transfer from an inclined heated flat plate placed beneath a porous medium of spherical particles was investigated numerically and experimentally. The effects of Reynolds number, angle of attack, and particle thermal conductivity on heat transfer were examined. The porous media used in the experiments were made of PVC, glass, and stainless steel spherical particles of 12 mm diameter. The results of the present work lead to the following conclusions:

1. For horizontal smooth flat plate, the local Nusselt number is relatively high at the leading edge, and it decreases to a uniform value towards the trailing edge. However, with inclined plates, the local coefficients are increased near the trailing edge of the plate.
2. For inclined smooth plate without porous medium, the maximum average Nusselt number enhancement ratio, $\overline{Nu}_{sm} / \overline{Nu}_{o}$, was about 1.239, and was obtained at $\alpha = 20^o$ and Re = 71927.
3. For the heated plate with or without porous medium, at the lower angles of attack ($\alpha \leq 20^0$) the average Nusselt number enhances with the increase in the angle of attack.
4. At the higher values of the angle of attack ($20^0 < \alpha \leq 30^0$) the average Nusselt number begins to decrease gradually with further increase in the angle of attack.
5. The experimental data that obtained for the average Nusselt number of a smooth flat plate without porous media was correlated as a function of Reynolds number and the angle of attack as follows:

$$\overline{Nu}_{sm} = 0.13\,Re^{0.703}\,(1+\sin\alpha)^{0.38}$$

This correlation was valid within the ranges of Reynolds number ($52000 \leq Re \leq 171000$), and the angle of attack ($0^o \leq \alpha \leq 20^o$). Also, the results that obtained from the model were utilized to correlate the average Nusselt number for the same case and conditions in the following equation:

$$\overline{Nu}_{sm} = 0.325\,Re^{0.6255}\,(1+\sin\alpha)^{0.5}$$

The present correlations were compared with the available previous correlations and good agreement was found.

6. The heat transfer is greatly augmented by the presence of the spherical particles. The local and average heat transfer coefficients increase with increasing the Reynolds number and the particle thermal conductivity.

7. For inclined plate with porous medium, the maximum enhancement ratio of the average Nusselt number, $\overline{Nu}_p/\overline{Nu}_o$, was about 3.10. This maximum enhancement ratio is obtained at $\alpha = 20^o$, Re = 71927 and using packed bed of stainless steel spheres.
8. An empirical correlation for the experimental average Nusselt number values of inclined flat plate in a porous medium was obtained as a function of Reynolds number (Re), the angle of attack ($\alpha$), and the particle-to-fluid thermal conductivity ratio $(k_s/k_f)$ as follows:

$$\overline{Nu}_p = 0.13\,Re^{0.703}\,(1+\sin\alpha)^{0.38}\,(k_s/k_f)^n$$

The exponent n = 0.1 for each of PVC and glass spheres, and n = 0.13 for stainless steel spheres porous medium. This correlation is valid within the present ranges of Reynolds number ($5.2x10^4 \le Re \le 1.71x\,10^5$), angle of attack ($0^o \le \alpha \le 20^o$), and the particle to fluid thermal conductivity ratio ($5.93 \le (k_s/k_f) \le 556$).

Also, the corresponding correlation for the numerical results that applied for the same ranges of the Reynolds number, inclination angle, and thermal conductivity ratio is:

$$\overline{Nu}_p = 0.108\,Re^{0.707}\,(1+\sin\alpha)^{0.678}\,(k_s/k_f)^{0.143}$$

9. Good agreement between the numerical code results and the experimental results for the all range of Reynolds number used in this investigation and for inclination angle ranges from $0^o$ to $20^o$.
10. From the numerical results, the fluid flow and heat transfer characteristics for the forced convection heat transfer from an inclined heated flat plate placed beneath a porous medium of spherical particles was obtained.

## NOMENCLATURE

| | |
|---|---|
| A | Surface area of the heated plate, $m^2$ |
| d | Particle diameter, m |
| F | Forchheimer coefficient |
| H | Duct height, m |
| h | Heat transfer coefficient, $W/m^2.K$ |
| $h_x$ | Local heat transfer coefficient, $W/m^2.K$ |
| $\bar{h}$ | Average heat transfer coefficient, $W/m^2.K$ |
| k | Turbulent kinetic energy, J/kg |
| $k_f$ | Thermal conductivity of fluid, W/m.K |
| $k_s$ | Thermal conductivity of solid spheres, W/m.K |
| L | Length of the test plate, m |
| $\overline{Nu}_o$ | Average Nusselt number for smooth horizontal plate without porous media |
| $\overline{Nu}_p$ | Average Nusselt number for plate with porous media |
| $\overline{Nu}_{sm}$ | Average Nusselt number for smooth inclined plate without porous media |
| $Nu_x$ | Local Nusselt number |
| $q_t$ | Total heat input to the main heater, W |
| $q''$ | Heat transferred per unit area (heat flux), $W/m^2$ |
| $R_m$ | Main heater electric resistance, Ω |
| Re | Reynolds number, = uL/ν |
| $S_\phi$ | Source term in Eq. (6). |
| $T_\infty$ | Free-stream temperature, $^o$C or K |
| $T_w$ | Surface temperature, $^o$C or K |
| u | Flow velocity, m/s |

$V_m$ Main heater voltage drop, V
u, v, w Velocity components in Cartesian coordinate system.
X Distance measured from the plate leading edge to the trailing edge, m
x, y, z Cartesian coordinates.

## Greek letters

$\alpha$ Angle of attack, deg.
$\gamma$ Reverse angle, deg.
$\nu$ Kinematic viscosity of the fluid, $m^2/s$
$\rho$ Density of the fluid, $kg/m^3$
$\pi$ Bulk porosity of the packed bed
$\Psi$ Yaw angle, deg.
$\phi$ Dependent variables (u, v, w, T, k, $\varepsilon$)
$\varepsilon$ Dissipation of kinetic energy, (k).

## Subscripts

f Fluid
m Main
o Smooth horizontal plate without porous medium
p Based on particle diameter or porous
s Solid spheres
sm Smooth inclined plate without porous medium

## REFERENCES

1. Sparrow, E. M., and Tien, K. K., "Forced Convection Heat Transfer at an Inclined and Yawed Square Plate-Application to Solar Collectors", ASME Journal of Heat Transfer, Vol. 99, pp. 507-512, 1977.
2. Imura, H ., Gilpin, R. R., and Cheng, K. C., "An Experimental Investigation of Heat Transfer and Buoyancy Induced Transition From Laminar Forced Convection to Turbulent Free Convection Over a Horizontal Isothermally Heated Plate", ASME Journal of Heat Transfer, Vol. 100, pp. 429-434, 1978.
3. El-Sayed, S. A., "Heat Transfer between an Air Stream and an Inclined Flat Plate", M. SC. Thesis, Cairo University, Faculty of Engineering, 1983.
4. Motwani, D. G., Gaitonde, U. N., and Sukhatme, S. P., "Heat Transfer from Rectangular Plates Inclined at Different Angles of Attack and Yaw to an Air Stream", ASME Journal of Heat Transfer, Vol. 107, pp. 307-312, 1985.
5. Shalaby, M. A., Araid, F. F., and Desoky, A. A., "Forced Convection Heat Transfer at Inclined and Yawed Rectangular Plate", Bulletin of the Faculty of Eng., El-Mansoura University, Vol.11, No.1, pp. M27-M39, 1986.
6. Shalaby, M. A., and Araid, F. F., "Heat Transfer and Flow Visualization of Separated Reattached Air Flow Over Reversed Rectangular Flat Plate", Mansoura Engineering Journal, Mansoura University, Vol. 12, No. 1, pp. M12-M22, 1987.
7. El-Shamy, A. R., "Air Flow and Heat Transfer Characteristics Over an Inclined Flat Plate", M. SC. Mech. Power Engineering, Faculty of Engineering, Cairo University, 1989.
8. El-Shamy, A. R., "Turbulent Boundary Layer and Heat Transfer Characteristics Over a Rough Flat Plate in Pressure Gradients", Ph. D. Thesis, Faculty of Engineering, Cairo University, 1994.
9. Abdel-Moneim, S. A., "An Experimental Study of Heat Transfer in a Turbulent Flow Over an Inclined Flat Plate", Proceedings of the 5th Int. Conference of Energy and Environment, Vol. 1, pp. 211-223, Cairo, Egypt, 1996.
10. Abdel-Moneim, S. A., El-Shamy, A. R., and Atwan, E. F., "Heat Transfer to a Turbulent Flow of Air Over an Inclined Rough Flat Plate", Engineering Research Journal, Helwan University, Faculty of Engineering, Mataria, Cairo, Vol. 50, pp. 13-26, 1996.
11. Afify, R. I., Abdellatif, O. E., and Berbish, N. S., "Influence of Free-Stream Turbulence on Turbulent Drag Reduction and Heat Transfer Enhancement Over Plates With Stream-Wise V-

Micro-Grooves", Engineering Research Journal, Helwan University, Faculty of Engineering, Mataria, Cairo, Vol. 94, pp. M23-M44, 2004.
12. Kamal, R. M., Mostafa, M. E., Abdel Aziz, S. S., "An Experimental Study of an Oblique Multiple Circular Air Jets Impingement on a Flat Plate", Eight International Congress of Fluid Dynamics and Propulsion, ICFDP8-EG-113, Sharm El-Shiekh, Sinai, Egypt, December 14-17, 2006.
13. Vafai, K., and Tien, C. L., "Boundary and Inertia Effects on Flow and Heat Transfer in Porous Media", Int. J. Heat Mass Transfer, Vol. 24, pp. 195-203, 1981.
14. Beckermann, C., and Viskanta, R., "Forced Convection Boundary Layer Flow and Heat Transfer Along a Flat Plate Embedded in a Porous Medium", Int. J. Heat Mass Transfer, Vol. 30, pp. 1547-1551, 1987.
15. Vafai, K., and Thiyagaraja, R., "Analysis of Flow and Heat Transfer at the Interface Region of a Porous Medium", Int. J. Heat Mass Transfer, Vol. 30, pp. 1391-1405, 1987.
16. Vafai, K., "Convective Flow and Heat Transfer in Variable-Porosity Media", Journal of Fluid Mechanics, Vol. 147, pp. 233-259, 1984.
17. Vafai, K., Alkire, R. L., and Tien, C. L., "An Experimental Investigation of Heat Transfer in Variable Porosity Media", ASME Journal of Heat Transfer, Vol. 107, pp. 642-647, 1985.
18. Poulikakos, D., and Renken, K. J., "Forced Convection in a Channel Filled With a Porous Medium Including the Effects of Flow Inertia, Variable Porosity, and Brinkman Friction", ASME Journal of Heat Transfer, Vol. 109, pp. 880-888, 1987.
19. Renken, K. J., and Poulikakos, D., "Experiment and Analysis of Forced Convective Heat Transport in a Packed Bed of Spheres," Int. J. Heat Mass Transfer, Vol. 31, No. 7, pp. 1399-1408, 1988.
20. Kaviany, M., "Boundary-Layer Treatment of Forced Convection Heat Transfer From a Semi-Infinite Flat Plate Embedded In Porous Media", ASME Journal of Heat Transfer, Vol. 109, pp. 345-349, 1987.
21. Renken, K. J., and Poulikakos, D., "Experiments on Forced Convection From a Horizontal Heated Plate in a Packed Bed of Glass Spheres," ASME Journal of Heat Transfer, Vol. 111, pp. 59-65, 1989.
22. Nakayama, A., Kokudai, T., and Koyama, H., "Non Darcian Boundary Layer Flow and Forced Convective Heat Transfer Over a Flat Plate in a Fluid-Saturated Porous Medium", ASME Journal of Heat Transfer, Vol. 112, pp. 157-162, 1990.
23. Afify, R. I., and Berbish, N. S., "Experimental Investigation of Forced Convection Heat Transfer Over a Horizontal Flat Plate in a Porous Medium", Journal of Engineering and Applied Science, Faculty of Engineering, Cairo University, Vol. 46, No. 4, pp. 693-710, 1999.
24. Luna, N., and Mendez, F., "Forced Convection on a Heated Horizontal Flat Plate With Finite Thermal Conductivity in a Non-Darcian Porous Medium", International Journal of Thermal Sciences, Vol. 44, No. 7, pp. 656-664, 2005.
25. Fluent Version 4.2 User's Guide, Fluent Incorporated, New Hampsier, 1993.
26. Polezhaev, Yu. V. and Seliverstov, E.M., "Universal Heat Transfer Model in porous media", Proceeding of 12th International Conference of Heat Transfer, France, 2002.
27. Kamiuto, K., Yee San San, and Matsuda, K., "Experimental Determination of Heat Transfer and Fluid Flow Characteristics of Open Cellular Porous Materials", Proceeding of 12th International Conference of Heat Transfer, France, 2002.

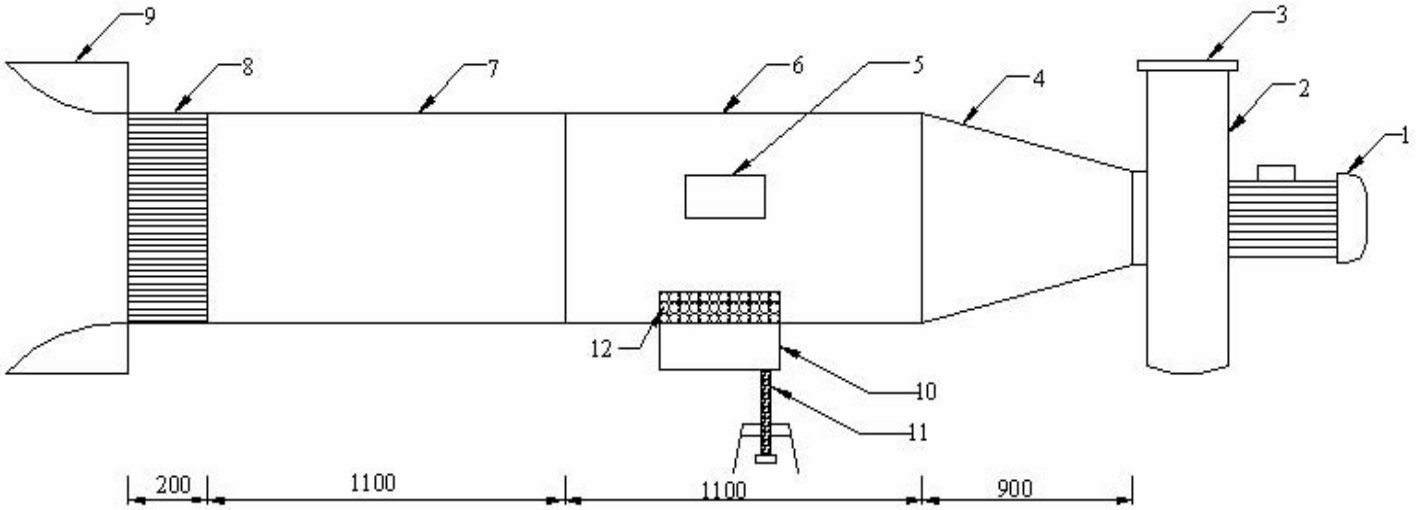


1- Electric Motor
2- Air Blower
3- Air Gate Control
4- Transformation Duct
5- Rectangular Opening
6- Test Section Duct
7- Upstream Duct
8- Honey Comb
9- Bell Mouth Intake
10- Heating Unit
11- Screw Mechanism
12- Porous Media

Fig.(1):Schematic diagram of the experimental set-up.

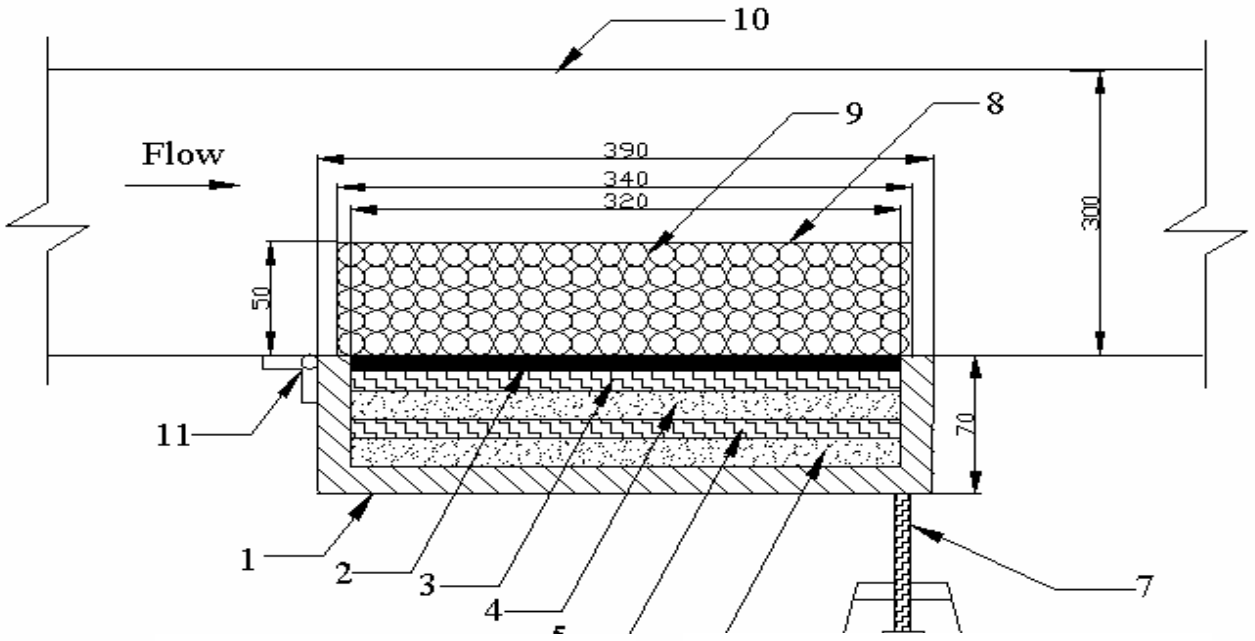


1- Wooden Frame
2- Heating Plate
3- Main Heater
4- Asbestos Insulation
5- Guard Heater
6- Asbestos Insulation
7- Screw Mechanism
8- Porous Cage
9- Porous Media
10- Test Section Duct
11- Hinges for Inclination

Fig.(2): Details of the test section.

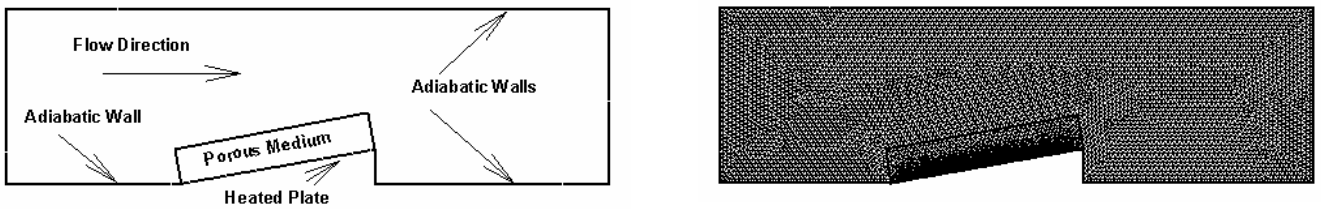


(a) Boundary conditions (b) Computational grid

Fig.(3): Schematic diagram of the problem

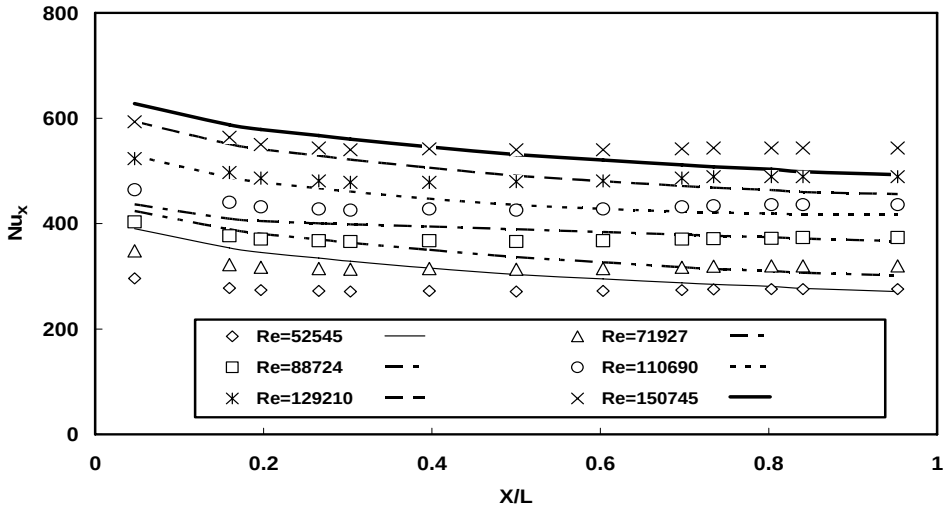


Fig.(4): Local Nusselt number versus X/L at different Reynolds numbers for horizontal plate without porous media, (Symbols: Experimental data, lines: CFD predictions)

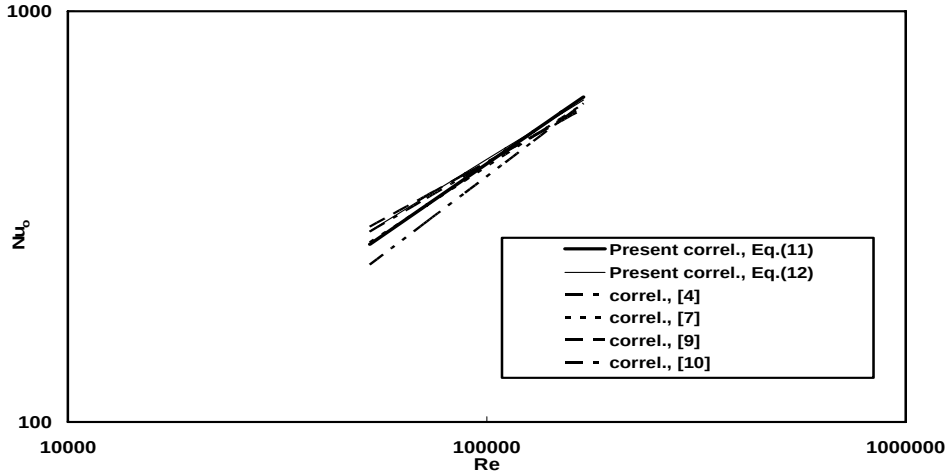


Fig.(5): Comparison between the present and previously published correlations for horizontal plate without porous media.

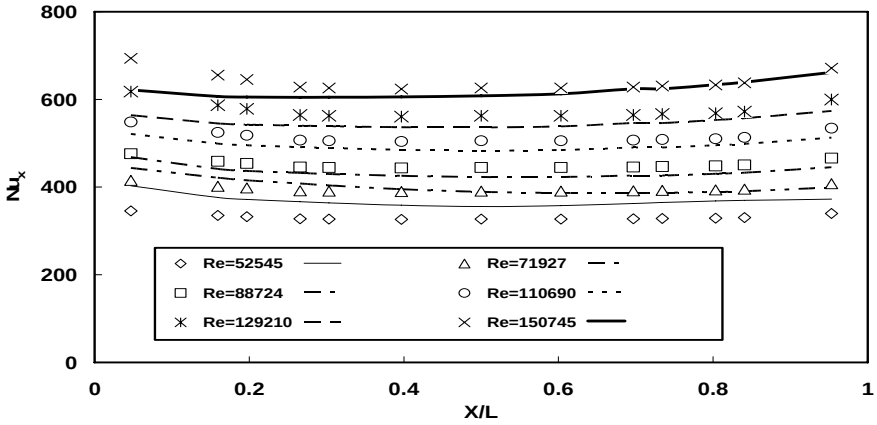


Fig.(6): Local Nusselt number distribution versus X/L at different Reynolds numbers for inclined plate without porous media ( $\alpha$=20 deg), (Symbols: Experimental data, lines: CFD predictions).

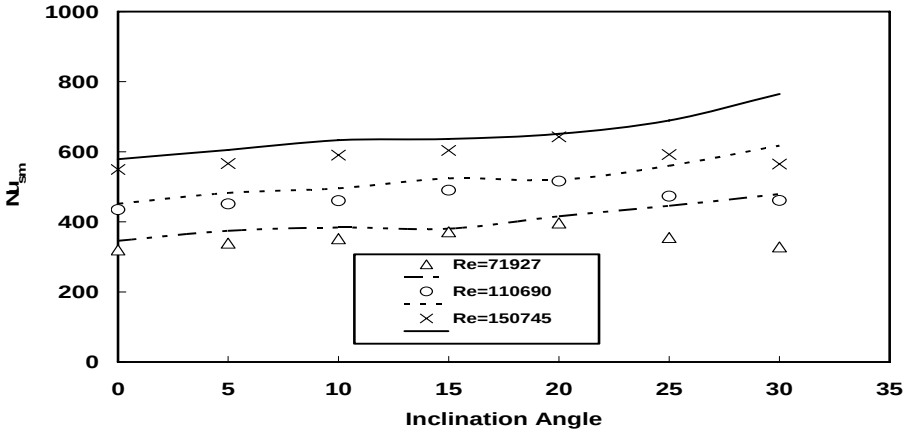


Fig.(7): The average Nusselt number versus the angle of attack for plate without porous media, (Symbols: Experimental data, lines: CFD predictions)

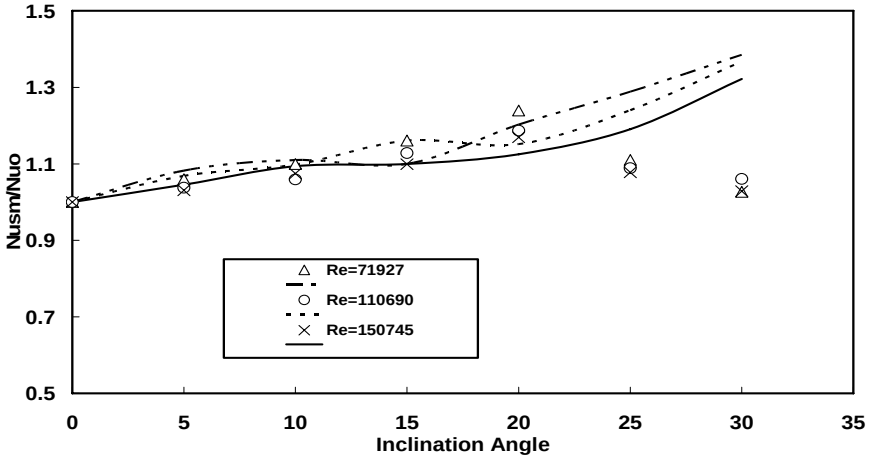


Fig.(8): Nusselt number enhancement ratio versus the angle of attack for plate without porous media, (Symbols: Experimental data, lines: CFD predictions)

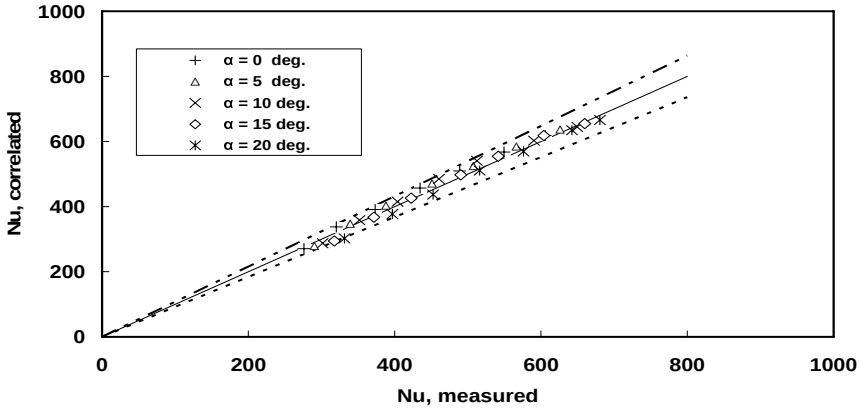


Fig.(9): Comparison of the present correlation with the present experimental data for plate without porous media.

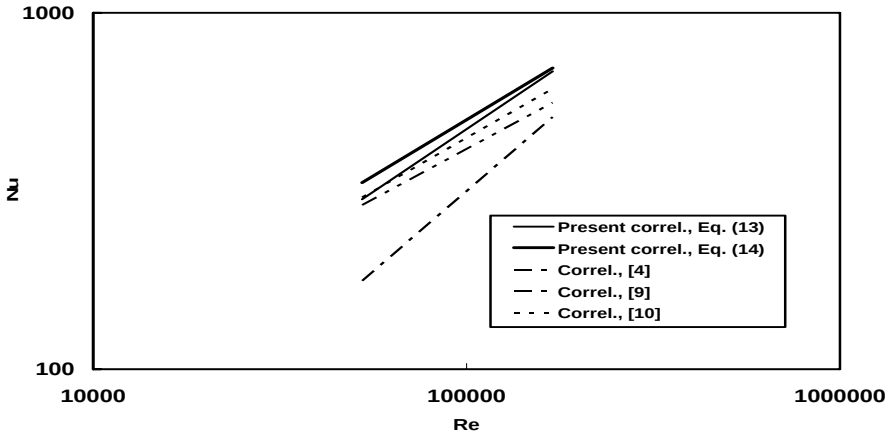


Fig.(10): Comparison between the present and previously published correlations for inclied plate without porous media (α =20 deg)

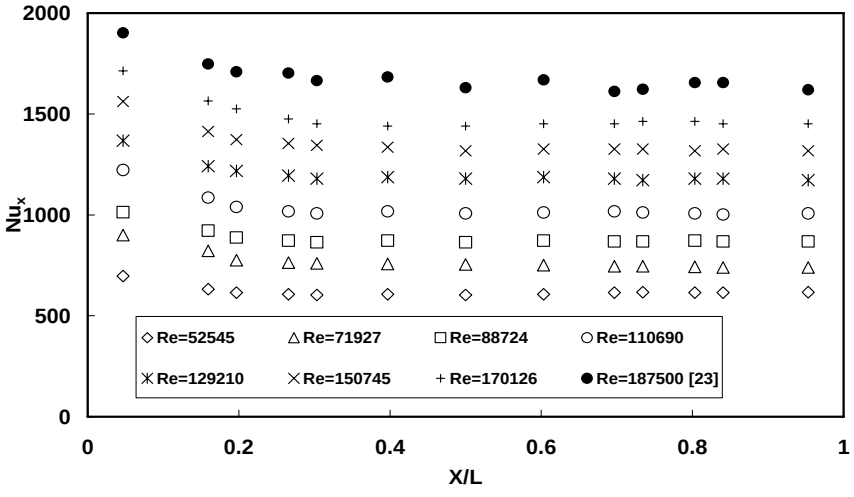


Fig.(11): Local Nusselt number versus X/L at different Reynolds numbers for plate with porous steel spheres (α= 0 deg)

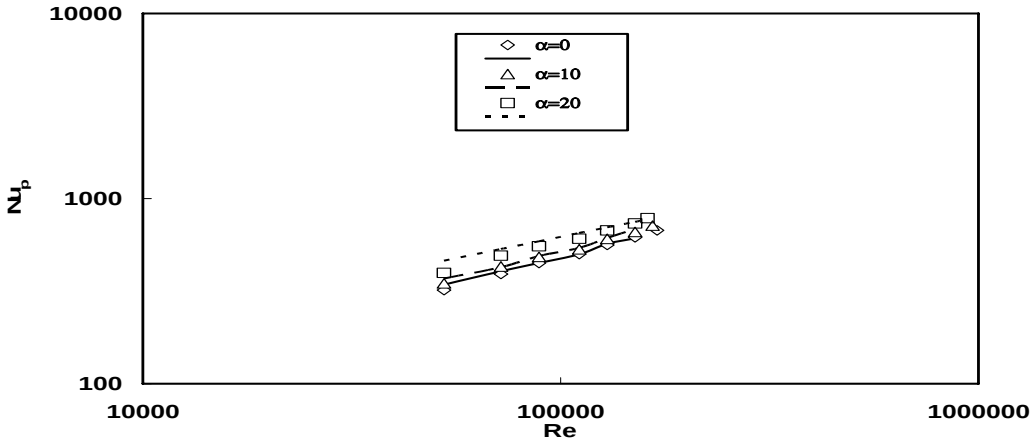


Fig.(12): The average Nusselt number versus Reynolds number for plate with porous PVC spheres (Symbols: Experimental data, lines: CFD predictions)

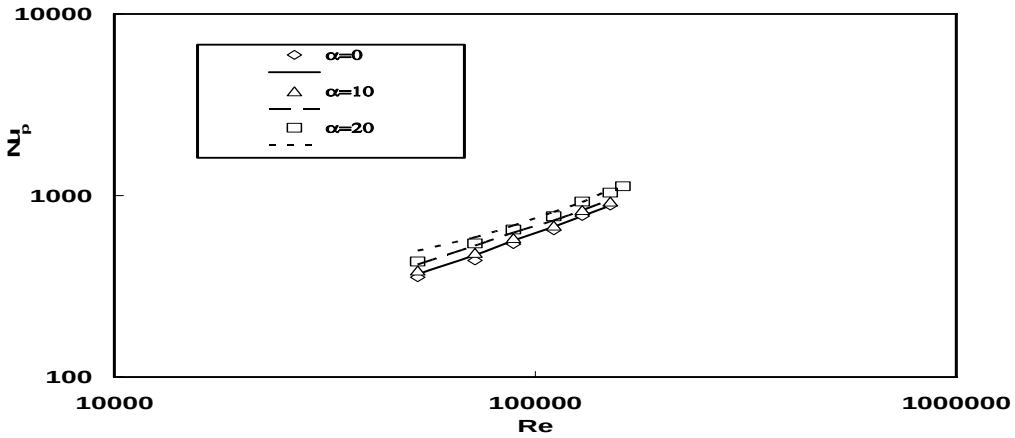


Fig.(13): The average Nusselt number versus Reynolds number for plate with porous glass spheres (Symbols: Experimental data, lines: CFD predictions)

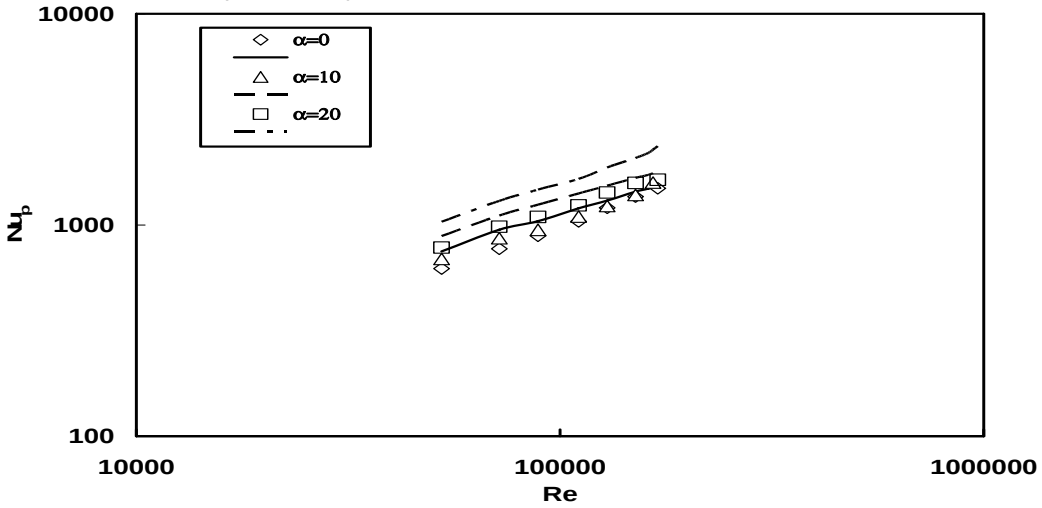


Fig.(14): The average Nusselt number versus Reynolds number for plate with porous steel spheres (Symbols: Experimental data, lines: CFD predictions)

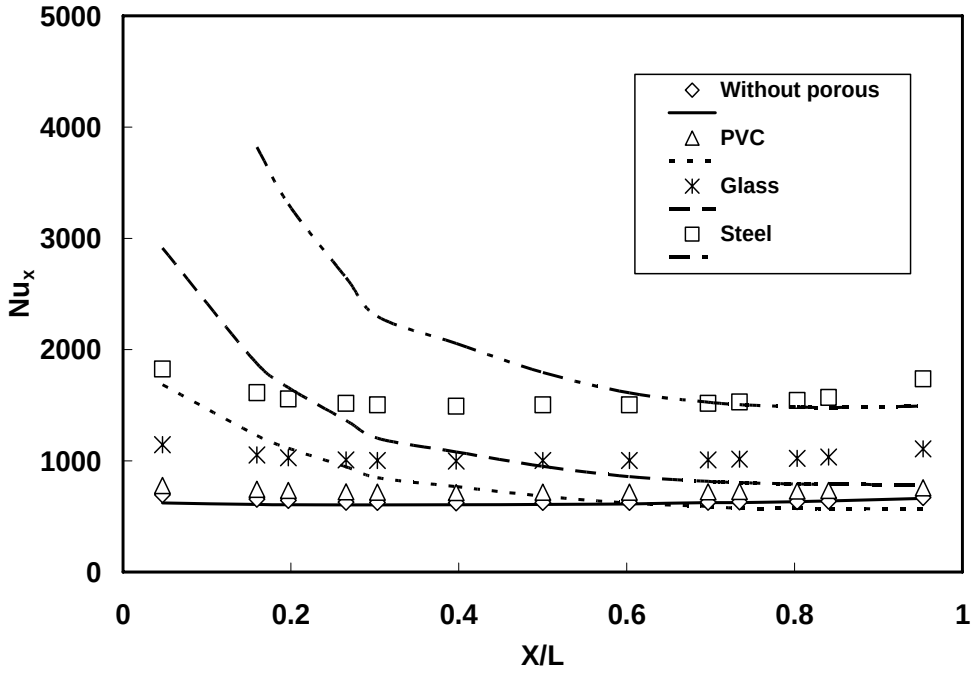


Fig.(15): Local Nusselt number versus X/L at different materials of the porous media for $\alpha = 20$ deg and Re = 150745, (Symbols: Experimental data, lines: CFD predictions)

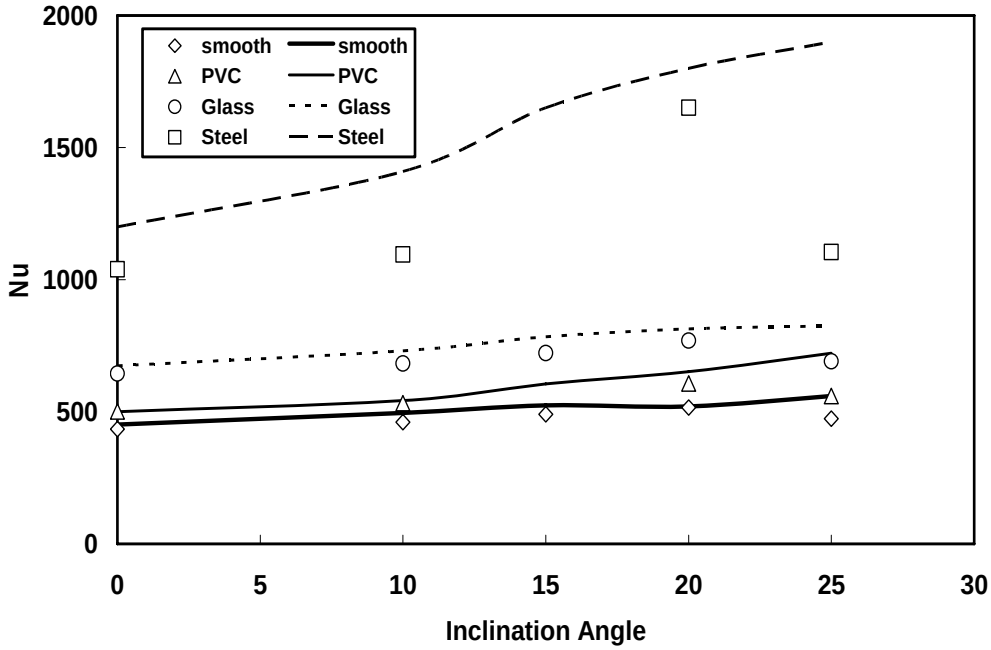


Fig.(16): The average Nusselt number versus the angle of attack for different materials of the porous media at Re = 110690, (Symbols: Experimental data, lines: CFD predictions)

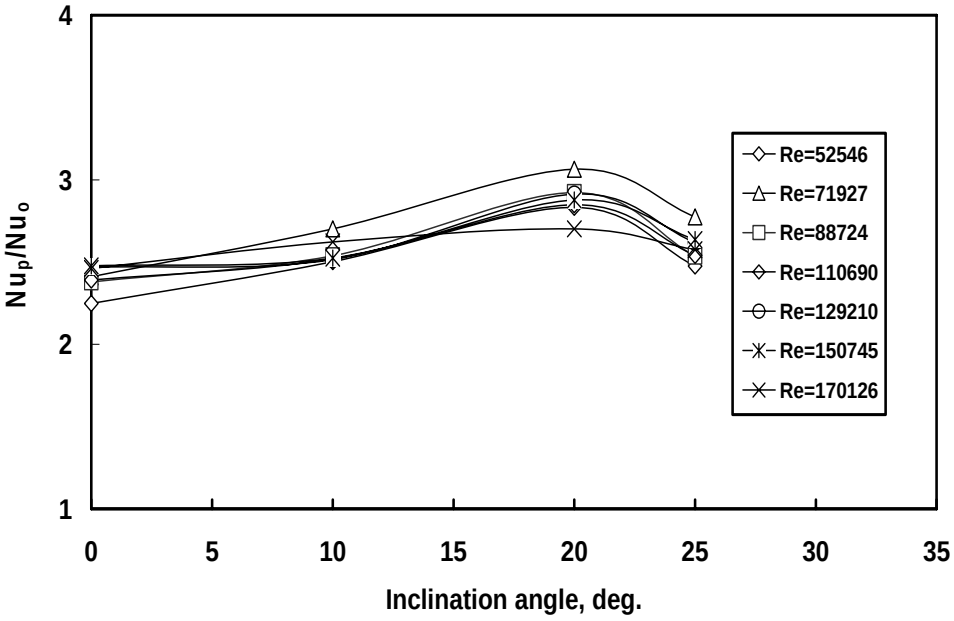


Fig.(17): Average Nusselt number enhancement ratio versus the angle of attack at different Reynolds numbers for steel spheres porous medium

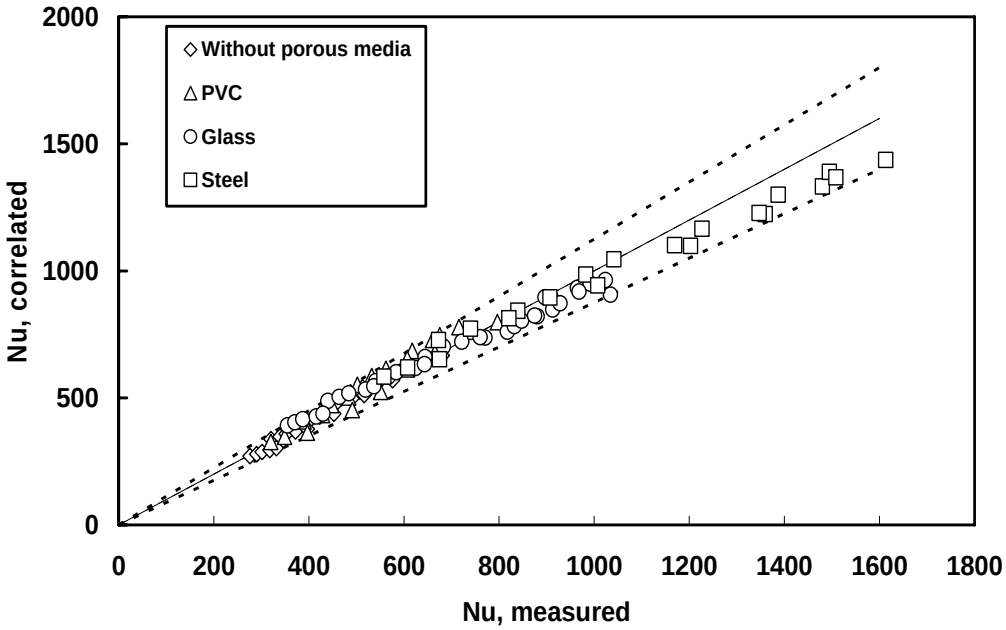


Fig.(18): Comparison of the present correlation with the present experimental data.

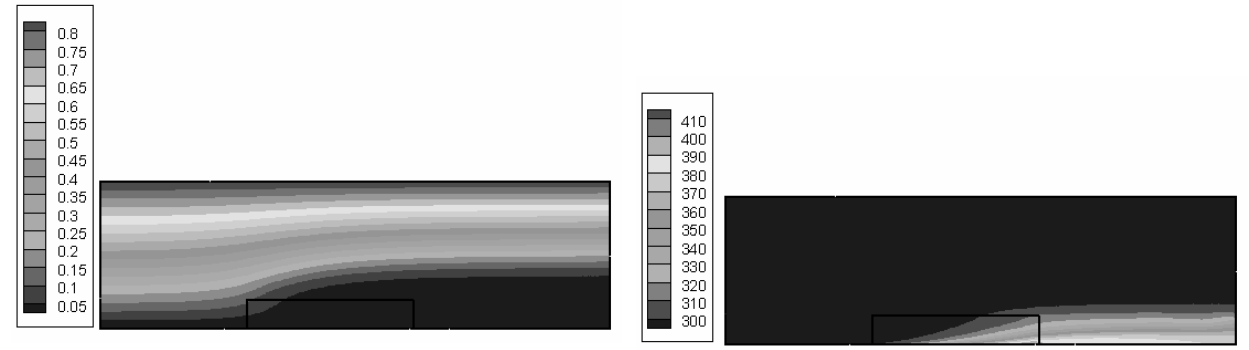


(a) Re=52546

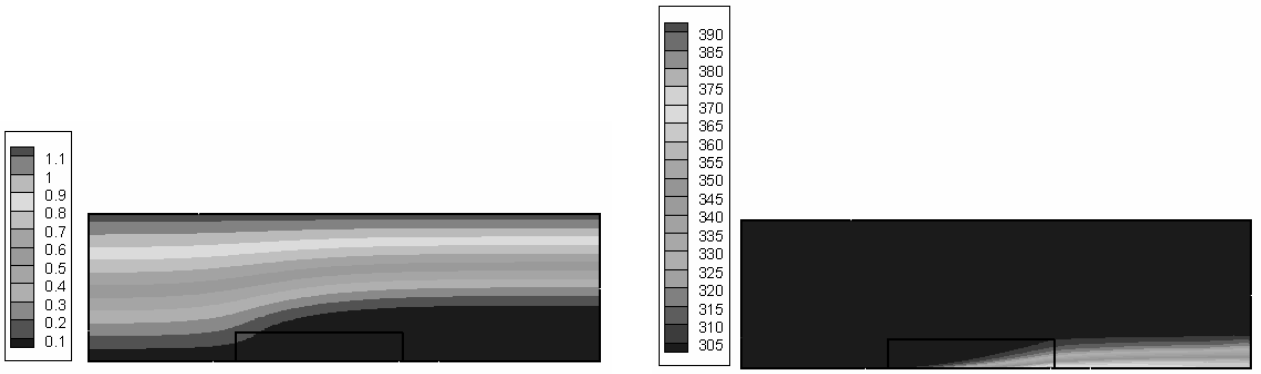


(b) Re= 71927

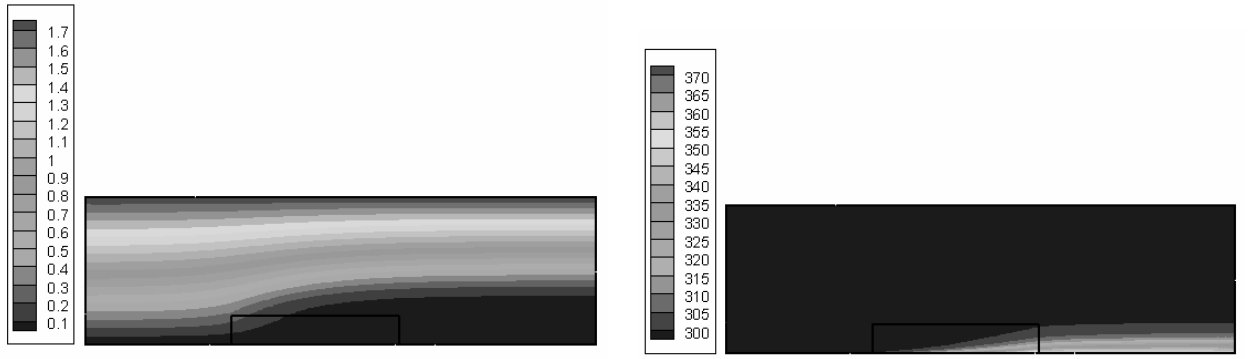


(c) Re= 110690

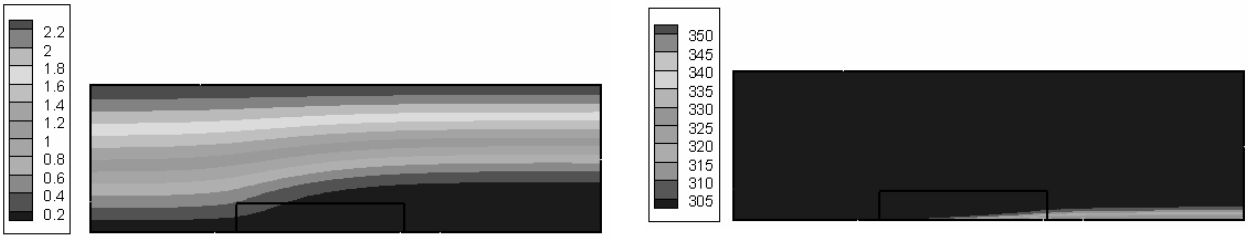


(d) Re= 150745

**Fig.(19): Stream function (left) and isotherms (right) contours for PVC porous spheres at $\alpha$=0 for different Reynolds number**

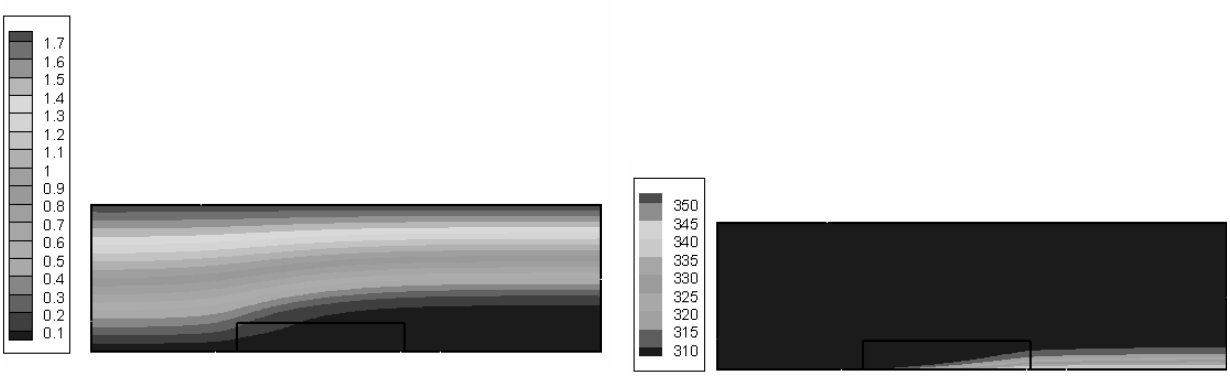


(a) $\alpha = 0^o$

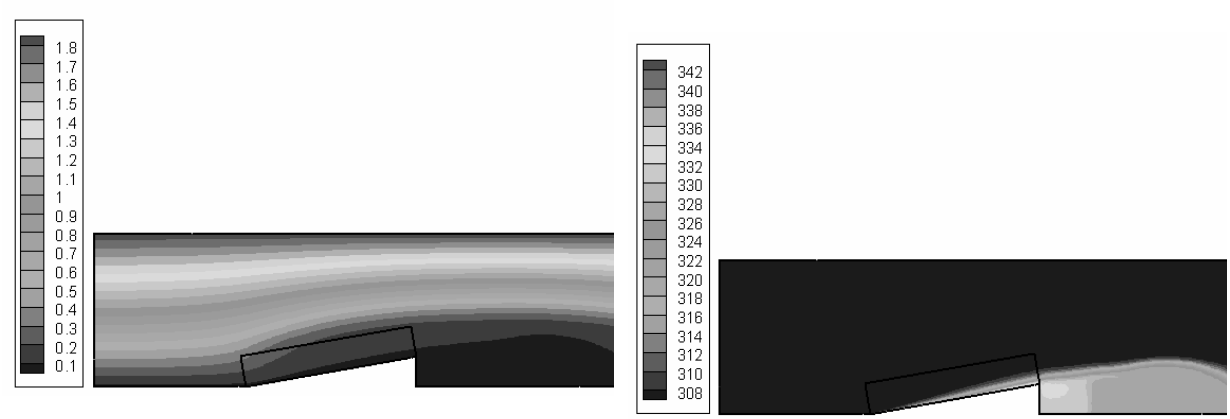


(b) $\alpha = 10^o$

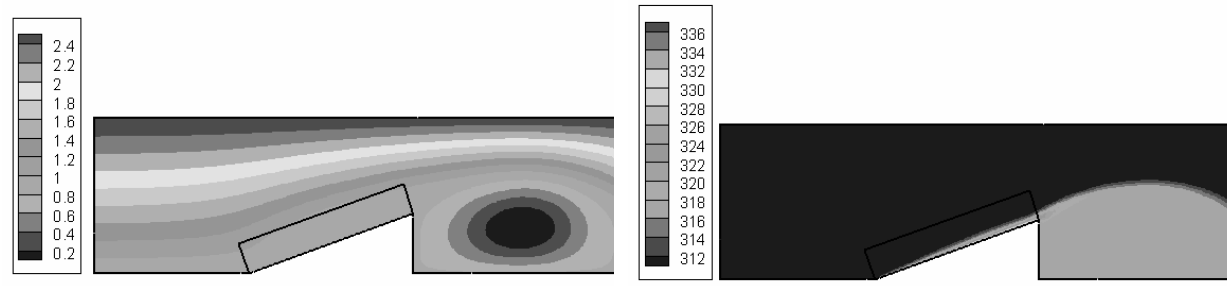


(c) $\alpha = 20^o$

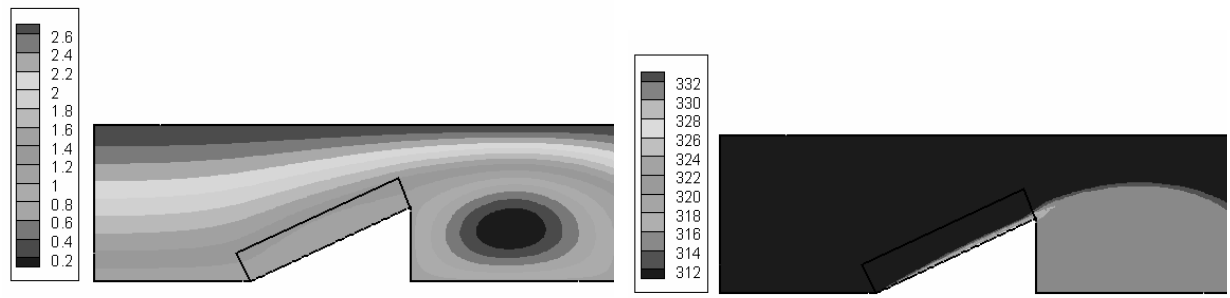


(d) $\alpha = 25^o$

**Fig.(20): Stream function (left) and isotherms (right) contours for glass porous spheres at Re=110690 for different inclination angles**

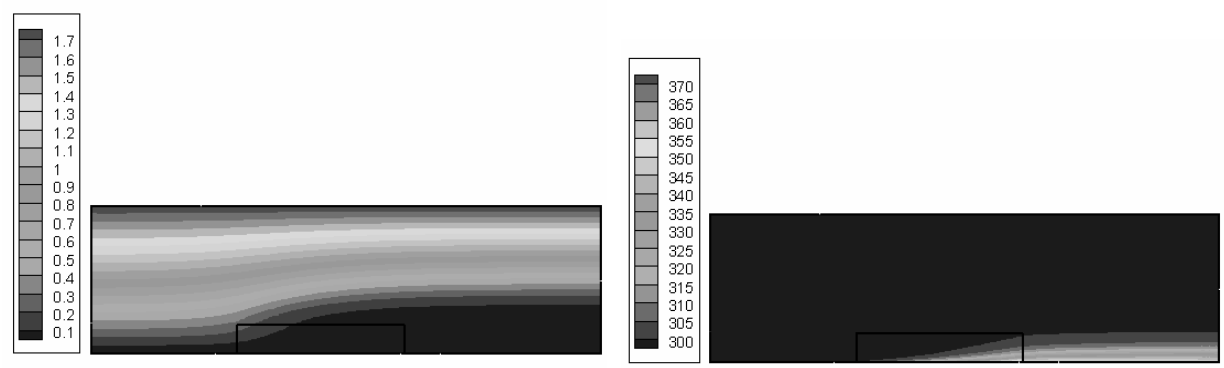


(a) PVC

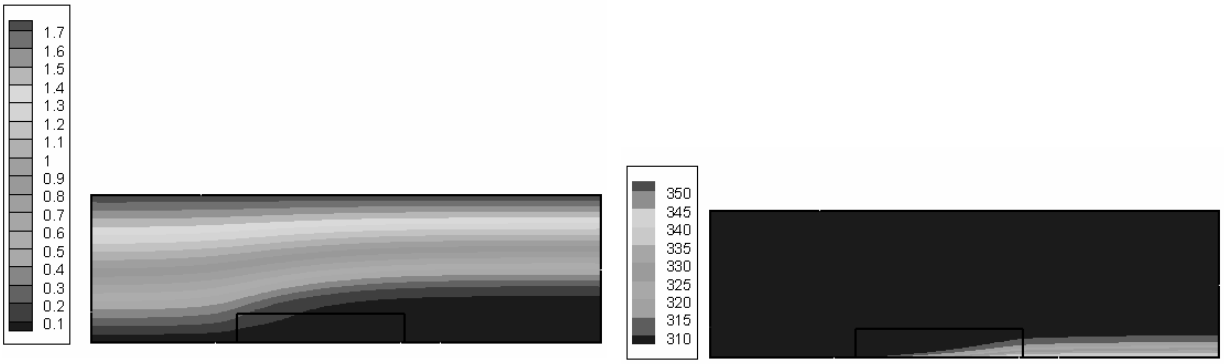


(b) Glass

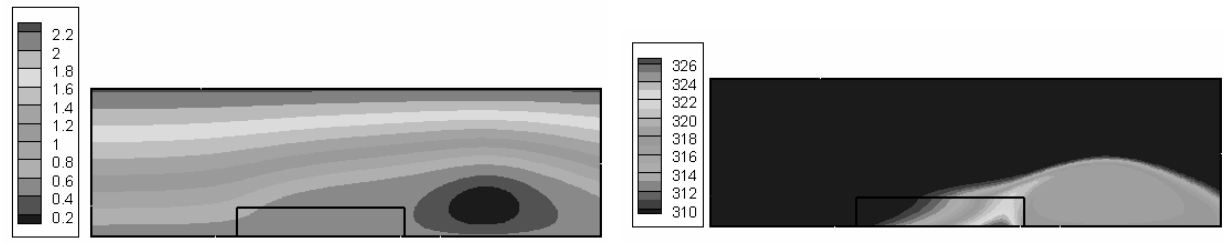


(c) Steel

**Fig.(21): Stream function (left) and isotherms (right) contours for PVC, glass, and Steel porous spheres at Re=110690 and $\alpha = 0^o$**